

Spin Susceptibility of a 2D Electron System in GaAs towards the Weak Interaction Region

Y.-W. Tan¹, J. Zhu¹, H. L. Stormer^{1,2,3}, L. N. Pfeiffer³, K. W. Baldwin³, and K. W. West³

¹*Department of Physics, Columbia University, New York, New York 10027*

²*Department of Applied Physics and Applied Mathematics,
Columbia University, New York, New York 10027*

³*Bell Labs, Lucent Technologies, Murray Hill, New Jersey 07974*

(Dated: November 7, 2018)

We determine the spin susceptibility χ in the weak interaction regime of a tunable, high quality, two-dimensional electron system in a GaAs/AlGaAs heterostructure. The band structure effects, modifying mass and g-factor, are carefully taken into accounts since they become appreciable for the large electron densities of the weak interaction regime. When properly normalized, χ decreases monotonically from 3 to 1.1 with increasing density over our experimental range from 0.1 to $4 \times 10^{11} \text{cm}^{-2}$. In the high density limit, χ tends correctly towards $\chi \rightarrow 1$ and compare well with recent theory.

PACS numbers: 71.18.+y, 73.40.-c, 73.43.Qt

I. INTRODUCTION

The recent interests in a possible correlated many particle state [1, 2, 3] at very low electron density of a two dimensional electron system (2DES) have sparked a series of experimental investigations in different materials.[4, 5, 6, 7, 8] In these experiments, the spin susceptibility, χ , which is proportional to the product of effective mass, m^* , and g-factor, g^* , usually deviates from its noninteracting “bare” band edge value, m_0g_0 , and increases drastically with decreasing electron density. The focus of these experiments is on the low density region, whereas χ has not been pursued to high densities. While we expect m^*g^* to approach m_0g_0 in the high density limit, the explicit behavior in the intermediate regime remains experimentally unresolved.

The density dependence of χ is usually expressed in terms of the dimensionless parameter, r_s . It is defined as the average e-e distance measured in units of the Bohr radius, which is also the ratio of Coulomb energy to Fermi energy. In 2D, $r_s \propto 1/\sqrt{n}$, the intermediate density regime resides at $r_s \sim 1$ and the high density regime at $r_s \rightarrow 0$. High r_s measurements of m^*g^* from different materials generally differ from each other and from theory. Most early calculations[9, 10, 11, 12] produced the sharp rise of χ at low densities, but differed quantitatively from experiments. Of those, data on very thin AlAs[8] quantum wells came closest to theory, probably since the latter omitted finite thickness effects. Indeed, recent calculation [13, 14, 15] have shown that most of the discrepancies arise from the finite thickness of the 2DES and the resulting modification of the Coulomb interaction. These calculations for χ extend far into the weak interaction regime, yet there are presently no data available to test their validity. An additional incentive for such measurement is the fact that an empirical relation for χ , observed in the low-density regime [7], when extrapolated to high density would imply vanishing χ , whereas one expects $\chi(n \rightarrow \infty) = 1$.

In this paper we provide high quality data on χ through the intermediate interaction regime and towards small r_s for comparison with recent, realistic theoretical calculations. Once the data are corrected for the energy dependence of band mass and g-factor, theory and experiment reach a remarkable level of accord and the data show the correct limiting behavior for large densities.

II. DEVICE STRUCTURE AND THE TILTED-FIELD MEASURING TECHNIQUES

Our primary sample is a heterojunction-insulated gate field effect transistor (HIGFET). It consists of a $5\mu\text{m}$ buffer GaAs layer grown by molecular beam epitaxy (MBE) on a (001) GaAs substrate. A subsequently grown, 200 period superlattice of $10\text{nm } Al_{0.33}Ga_{0.67}As$ and 3nm GaAs acts as a diffusion barrier. It is followed by $5\mu\text{m}$ of undoped GaAs, which functions as the channel. This layer is covered by 5nm of AlAs and $4\mu\text{m}$ of $Al_{0.33}Ga_{0.67}As$, being the dielectric material, topped by 25nm of heavily doped GaAs, which serves as the gate. The specimen is processed into a $600\mu\text{m}$ square mesa. We use standard photolithography to define fifteen Ni-Ge-Au contact pads. Our specimen has mobilities as high as $1 \times 10^7 \text{cm}^2/\text{Vs}$. The density, n , can be tuned by varying the gate voltage, V_g . For this sample, $n(10^{10} \text{cm}^{-2}) = 0.15 + 16 \times V_g(V)$. Such a HIGFET allows us to measure a wide range of densities in a single specimen, eliminating sample to sample parameter fluctuations. For our sample, which has a density range spanning from 0.1×10^{11} to $4 \times 10^{11} \text{cm}^{-2}$, the r_s value can be tuned from 0.9 to 6, covering a wide range of e-e interaction strength.

All measurements were performed in a dilution refrigerator with a base temperature of $\sim 30\text{mK}$. The sample was mounted on a rotating sample holder to control separately the total magnetic field, B_{tot} , and the field, B_{\perp} , perpendicular to the 2DES. We used conventional low

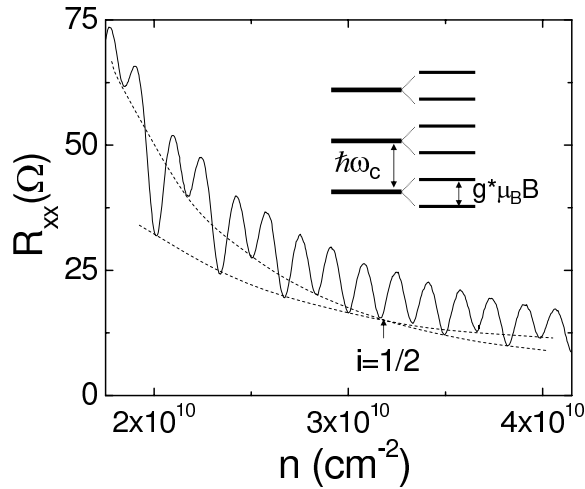


FIG. 1: A typical gate sweep trace showing the coincidence condition for $i = 1/2$, at $B_{\perp} = 0.07T$ and tilt angle $= 86.5^{\circ}$. The arrow indicates the density for coincidence to be $n = 3.3 \times 10^{10} \text{ cm}^{-2}$. inset: schematic diagram for the $i = 1/2$ coincidence, where spin splittings from the same and neighboring Landau levels are evenly spaced.

frequency ac lock-in techniques with excitation currents ranging from 1nA to 100nA, chosen to avoid sample heating.

We determine the spin susceptibility, χ , by the tilted field method[16], in the context of GaAs HIGFETs[7]. We briefly review the method, referring to Ref.[7] for details: For a 2D system in a magnetic field, the spacing between Landau levels, $\hbar\omega_c = e\hbar B_{\perp}/m^*$, depends on the perpendicular field B_{\perp} , while the Zeeman energy $\Delta E_z = g^*\mu_B B_{tot}$, depends on the total magnetic field, B_{tot} . When $|g^*\mu_B B_{tot}| = i\hbar\omega_c$, where the coincidence index, i , is an integer or a half-integer[17], the Landau levels of the spin-up and spin-down electrons form a ladder of evenly spaced energy levels. A schematic diagram of evenly spaced energy levels is shown for $i = 1/2$ as an insert to figure 1.

The coincidence condition has a clear signature in the oscillation amplitudes of the magnetoresistance. In a density sweep at fixed θ and B , and assuming m^* and g^* not to depend on density, such evenly spaced energy levels reveal themselves as uniform oscillation of uniform amplitudes. However, in general, m^* and g^* depend on electron density and therefore such equal amplitude oscillations only appear at a particular density, n . Only at this particular n the value of $m^*g^* = 2im_0B_{\perp}/B_{tot}$. As an example, fig. 1 shows such a sweep for the $i=1/2$ coincidence.

III. RESULTS

Fig. 2 shows the so determined n -dependent values of m^*g^* . Our data cover low r_s values and, hence, persist into the low interaction regime, whereas earlier data by

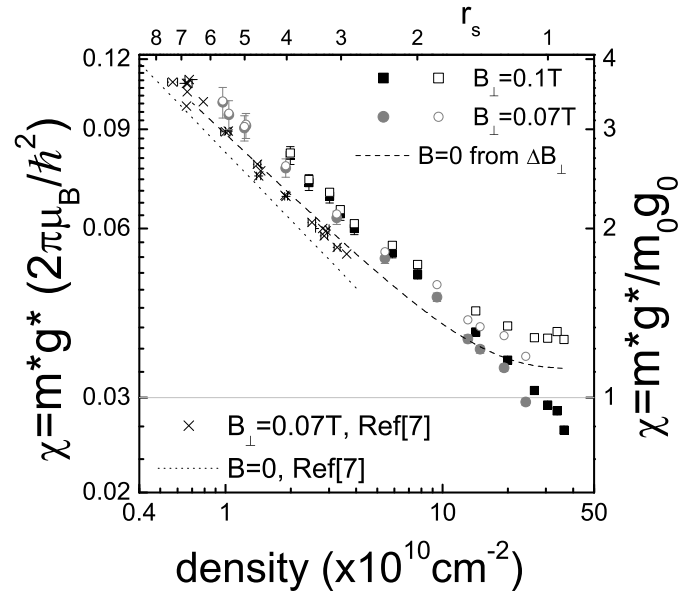


FIG. 2: Spin susceptibility χ versus electron density. Black squares are measurements for $i = 1/2$ in perpendicular field, $B_{\perp} = 0.1T$; grey circles are data for $i = 1/2$ and $B_{\perp} = 0.07T$. The error bars in χ represents the uncertainties in angle. Errors in density are smaller than the symbol size. Open symbols represent data of same-shaped filled symbols after corrected for band structure effects. The extrapolation of χ to $B_{tot} \rightarrow 0$ is plotted as a dashed line(see text). After this correction the right scale becomes effectively $\chi = m^*g^*/m_b g_b$, which is used in fig. 4. Low density data from ref.[7] are plotted for comparison.

Zhu et al.(also shown) are limited to the high interaction regime($r_s \gtrsim 3$). Our data were taken in two different perpendicular fields $B_{\perp} = 0.1T$ and $B_{\perp} = 0.07T$, both using the coincidence index $i = 1/2$. The error bars in the y-direction represent the uncertainties in angle measurements. For comparison, we also show the low-density data for the $i = 1/2$ taken at $B_{\perp} = 0.07T$ from Ref.[7]. The small difference between our $B_{\perp} = 0.07T$ data and theirs is most likely due to a slightly thinner wave function thickness owing to the extra AlAs layer in our sample(see above).

To put the main features of our data in perspective, we first follow the conventional way of normalizing the χ data simply to the literature band edge values of m_0g_0 . We provide this scale on the right side of Fig.2 Clearly the spin susceptibility decreases monotonically with increasing density from 3.4 to 0.88 for electron densities from 0.1×10^{11} to $4 \times 10^{11} \text{ cm}^{-2}$. On this log-log plot, the data from each B_{\perp} follow a power law behavior with a similar slope as observed earlier in the low density regime [7]. Obviously the data drop below $\chi = 1$ for high densities, which is unphysical and contradicts all theoretical predictions. However, bandstructure effects, which modify the “bare” mass and g-factor of the carriers, alter the power-law and prevent this from occurring. While such effects

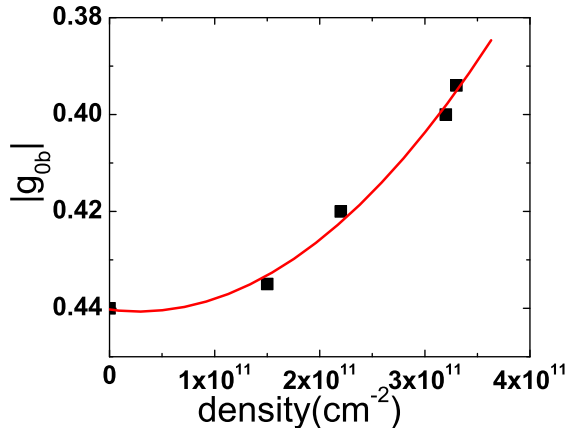


FIG. 3: Data and fit for coefficient g_{ob} from literature values[23, 25, 26] (see text and equation (1)).

are negligible in the low density regime, they are appreciable at higher densities and need to be corrected for. In particular, in GaAs, the band mass m_b increases with increasing density, while the magnitude of the g-factor, $|g_b|$, decreases, with the latter being dominant.

IV. CORRECTIONS FOR BAND STRUCTURE EFFECTS

The density dependence of the electron band mass in a 2DES in GaAs due to band nonparabolicity has been widely studied and can be readily calculated [21]. For our density range 0.1×10^{11} to $4 \times 10^{11} \text{ cm}^{-2}$, the enhancement of m_b grows from 0.3% to 5%. The density dependence of the g -factor is more complex. In a 2DES, this dependence was first observed by Stein et al. [22] using Electron Spin Resonance (ESR) and was later studied systematically via ESR by Dobers et al.[23]. They deduced an empirical formula $g_b(B, N) = g_{b0} - c(N + 1/2)B$, where N is the Landau level index, B is the magnetic field, and g_{b0} and c are two coefficients that may change with electron density. The observation was explained theoretically [24] as a combination of nonparabolicity of the band structure and an increase of the penetration of the electron wavefunction into the AlGaAs layer. Since the g -factor of $\text{Al}_x\text{Ga}_{1-x}\text{As}$ changes considerably with Aluminum concentration and has a different sign from g_0 in GaAs, the magnitude of the g -factor shrinks with increasing penetration of the electron wavefunction. In order to correct our data, we use the existing measurements[23, 25, 26] of g_{b0} and c values from samples with electron densities from $n = 1.5 \times 10^{11}$ to $n = 3.3 \times 10^{11} \text{ cm}^{-2}$. Adding $g_{b0} = -0.44$ for $n \rightarrow 0$, we interpolate and achieve the phenomenological dependence,

$$g_{b0}(n) = -0.44 - 2.75 \times 10^{-4}n + 4.98 \times 10^{-5}n^2, \quad (1)$$

where n is in $10^{10}/\text{cm}^{-2}$ (see fig.3). The coefficient c is assumed constant, $c=0.012$, since it hardly varies in

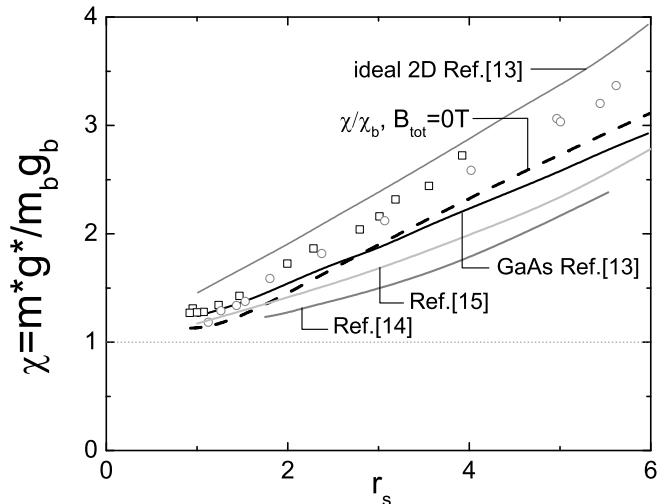


FIG. 4: Normalized spin susceptibility enhancement χ versus r_s . The open symbols are data corrected for band structure effects due to nonparabolicity. The extrapolation to $B_{tot} = 0$ is shown as a dashed line as in fig.2. m_b and g_b denote the bare m and g values after corrected for band structure effect. The solid curves of different grey scale are theoretical calculations from ref.[13, 14, 15]. The topmost curve is for a zero-thickness 2DES, whereas all other solid curves are for finite thickness GaAs systems.

Ref.[23]. While Dobers et al. used an Al concentration of $\sim 35\%$, the interface in our sample consists of 100% Al. From band structure calculations we can estimate that such a 100% Al concentration at the interface reduces the g -factor renormalization by $\sim 1/2$ as compared to $\sim 35\%$ Al. When combined with a smaller penetration into the AlAs layer, the final enhancement m^*g^*/m_bg_b is affected by less than 4% at our highest r_s and has no observable effect for $r_s > 1.5$. A similar estimate yields a variation of c by less than 1% from $\text{Al}_{0.35}\text{Ga}_{0.65}\text{As}/\text{GaAs}$ to AlAs/GaAs . These calculations are approximate. However, we deem them sufficient since their impact on our data resides within the experimental error bar.

The open symbols in fig. 2 represent all our χ data corrected for the density dependence of mass and g -factor. As required, all data remain above $\chi = 1$ and they seem to be levelling off as n increases. Since we have been working with a small spin polarization ($i = 1/2$) our data can be assumed to be close to the unpolarized(*i.e.* $B_{tot} \rightarrow 0$) case, which is the condition used in most theoretical calculations and therefore of importance for comparisons with experiment. Based on the B_{tot} -dependence of our low-density data we can actually provide an extrapolation scheme to $B_{tot} \rightarrow 0$, which, since it is a small correction, should hold over the extended high density range provided here.

We observe that the $B_{\perp} = 0.1T$ data and the $B_{\perp} = 0.07T$ data are slightly offset from each other in the vertical direction. In particular, at lower densities both follow the previously observed powerlaw, which had allowed

for a simple extrapolation scheme[7] to $B_{tot} \rightarrow 0$. This extrapolation, based on different coincidence indices, i , can directly be translated to different B_{\perp} and identical $i = 1/2$ as is the case in the present measurements (see footnote [18]). The result is a constant multiplicative factor, which appears as a small downward shift on our log-log plot of Fig. 2 is shown as a dashed line. While this extrapolation scheme is derived in the range of the powerlaw dependence between χ and n of our data, we expect it to apply approximately also in the range of saturating χ towards higher densities.

An enhancement of m^* and a deduced increase of g^* by a high in-plane magnetic field has been reported by Tutuc et al.[20] According to their observations, the mass enhancement for our largest in-plane field of $3.9T$, at density $3.6 \times 10^{11} cm^{-2}$, is approximately 8%. Extrapolating their g^* enhancement to this density and field, we find it to be less than $\sim 2\%$. Our χ enhancement from the $B \rightarrow 0$ extrapolation is $\sim 9\%$, which is close to the overall $\sim 10\%$ increase deduced from Ref.[20]. This supports that our method, which *extrapolates* the spin susceptibility to vanishing B field, $\chi_{B \rightarrow 0} = m^* g^* / m_0 g_0$, is not sensitive to in-plane field effects on m^* and g^* .

Fig 4 shows our final results as χ versus r_s , rather than versus density, for better comparison with theory. The symbols and lines refer back to fig.2. The data points as well as the extrapolated curve show the correct limiting behavior of $\chi \rightarrow 1$ as $r_s \rightarrow 0$ as a consequence of the correction of the data for band structure effects. Without such correction, the χ data would have fallen below $\chi = 1$, which would be clearly unphysical.

V. COMPARISON WITH THEORIES

Finally, we can compare our data with theory. In the past two decades, there have been several calculations of the spin susceptibility χ , but most of them evaluate χ in the limit of zero polarization in an ideal 2DES. A figure summarizing those theoretical results can be found in Ref.[9]. The calculations from different techniques are in rather good agreement for $r_s < 3$ but deviate considerably for large r_s . In the same regime, measurements of χ in different 2DESs have also shown considerable discrep-

ancies. A recent report of dePalo et al, attributes many of these discrepancies to the finite thickness of the real 2DES and variations of this thickness between 2DESs from different material systems. For comparison with our data, extrapolated to $B \rightarrow 0$ (dashed line), we have included in fig.4 the zero thickness result and the finite thickness result for GaAs from ref[13]. The calculations from Zhang and Das Sarma[14] using an improved RPA and Dharma-wadana[15] using a CHNC method both reside further below our data.

As can be seen from fig.4, our experimental data and the theoretical calculations for a realistic 2DES in GaAs show rather good agreement. For high r_s values, this had been pointed out before[13]. Here we show that after appropriate correction for band structure effects, one also achieves good agreement in the intermediate interaction regime ($r_s \sim 1$) and obtains the correct trend for $r_s \rightarrow 0$.

VI. CONCLUSION

In conclusion, our data on the spin susceptibility of a 2DES in GaAs over a very wide of electron densities, covering r_s values from strong electron interactions ($r_s \sim 6$) through the intermediate interaction regime ($r_s \sim 1$), and into the low interaction regime show the correct trends for the limiting behavior ($r_s \rightarrow 0$) of this quantity. Only when theory takes into account the finite thickness of the real 2DES and experiment is corrected for band structure effects, a rather good agreement between data and calculation is reached over the whole range of r_s of this study. Our work highlights the fact that subtleties of the real 2DES need to be taken into account when comparison with theoretical calculations are being made.

Acknowledgments

The authors acknowledge Dr. Roland Winkler for discussion. This work is supported by NSF under DMR-03-52738, by the DOE under DE-AIO2-04ER46133, and by a grant of the W. M. Keck Foundation.

-
- [1] F. Bloch, Z. Phys. **57**, 545 (1929).
 - [2] E. C. Stoner, Proc. R. Soc. London A **165**, 372 (1938).
 - [3] E. Wigner, Phys. Rev. **46**, 1002 (1934).
 - [4] A. A. Shashkin, S. V. Kravchenko, V. T. Dolgoplov, and T. M. Klapwijk, Phys. Rev. Lett. **87**, 086801 (2001).
 - [5] V. M. Pudalov, M. E. Gershenson, H. Kojima, N. Butch, E. M. Dizhur, G. Brunthaler, A. Prinz, and G. Bauer, Phys. Rev. Lett. **88**, 196404 (2002).
 - [6] E. Tutuc, S. Melinte, and M. Shayegan, Phys. Rev. Lett. **88**, 036805 (2002).
 - [7] J. Zhu, H. L. Stormer, L. N. Pfeiffer, K. W. Baldwin, and K. W. West, Phys. Rev. Lett. **90**, 056805 (2003); Phys. E **22**, 228 (2004).
 - [8] K. Vakili, Y. P. Shkolnikov, E. Tutuc, E. P. De Poortere, and M. Shayegan, Phys. Rev. Lett. **92**, 226401 (2004).
 - [9] C. Attacalite, S. Moroni, P. Gori-Giorgi, and G. B. Bachelet, Phys. Rev. Lett. **88**, 256601 (2002), and references therein.
 - [10] B. Tanatar and D. M. Ceperley, Phys. Rev. B **39**, 5005 (1989).
 - [11] S. M. Reimann, M. Koskinen, M. Manninen, and B. R. Mottelson, Phys. Rev. Lett. **83**, 3270 (1999).

- [12] S. Yarlagadda and G. F. Giuliani, Phys. Rev. B **40**, 5432 (1989).
- [13] S. DePalo, M. Botti, S. Moroni, and G. Senatore Phys. Rev. Lett. **94**, 226405 (2005).
- [14] Y. Zhang and S. Das Sarma Phys. Rev. B **72**, 075308 (2005).
- [15] M. W. C. Dharma-wardana (2005), cond-mat/0503246.
- [16] F. F. Fang and P. J. Stiles, Phys. Rev. **174**, 823 (1968).
- [17] The g-factor does depend on Landau level filling and hence this equation is only approximately observed. However, since we are working at relatively high densities, low perpendicular field and in high Landau levels, the oscillation amplitude of the g-factor is small and we can assume it to be constant near the Fermi surface.
- [18] Powerlaw fits to our two data sets at low n and different B_{\perp} yield $m^*g^*/m_0g_0(B_{\perp} = 0.1T) = 3.40n^{-0.365}$ and $m^*g^*/m_0g_0(B_{\perp} = 0.07T) = 3.27n^{-0.365}$. Based on ref.[7], we take the prefactor in the power law to be linear in total field B_{tot} as $3.40 = a + bB_{tot}^{0.1T}$, and $3.27 = a + bB_{tot}^{0.07T}$. Using $i = 1/2 = m^*g^*\mu_B B_{tot}/e\hbar B_{\perp}$ to link B_{\perp} with B_{tot} we arrive at $B_{\perp} = 0.0295(m^*g^*/m_0g_0)B_{tot}$, yielding $B_{tot}^{0.1T}/B_{tot}^{0.07T} = 1.37$. Solving for $a = [3.40 - (B_{tot}^{0.1T}/B_{tot}^{0.07T})3.27]/[1 - (B_{tot}^{0.1T}/B_{tot}^{0.07T})] = 2.92$, and applying the solutions to $m^*g^*/m_0g_0 = (a + bB_{tot})n^{-0.365}$ we arrive at $\chi_{B \rightarrow 0} = 2.92n^{-0.365}$ as $B_{tot} \rightarrow 0$ for low n . This modified prefactor leads to a vertical shift and is applied to all data to yield $\chi(B_{tot} \rightarrow 0)$.
- [19] The empirical relationship between n and χ includes an n -dependent finite thickness effect due to the softening of the Coulomb interaction.
- [20] E. Tutuc, S. Melinte, E. P. De Poortere, M. Shayegan, and R. Winkler, Phys. Rev. B **67**, 241309(R) (2003).
- [21] S. Das Sarma and B. A. Mason, Phys. Rev. B **31**, R1177 (1985).
- [22] D. Stein, K. v. Klitzing, and G. Weimann, Phys. Rev. Lett. **51**, 130 (1982).
- [23] M. Dohers, K. v. Klitzing, and G. Weimann, Phys. Rev. B **38**, 5453 (1988).
- [24] G. Lommer, F. Malcher, and U. Rossler, Phys. Rev. B **32**, R6965 (1985).
- [25] M. Dohers, Surf. Sci. **229**, 126 (1990).
- [26] R. Meisels, K. Dybko, F. Ziouzia, F. Kuchar, R. Deutschmann, G. Abstreiter, G. Hein, and K. Pierz, Phys. E **10**, 57 (2001).